Chinese Chemical Letters 32 (2021) 2342–2346

Contents lists available at ScienceDirect

Chinese Chemical Letters

journal homepage: www.elsevier.com/locate/cclet

Communication

A millimeter-sized negatively charged polymer embedded with molybdenum disulfide nanosheets for efficient removal of Pb(II) from aqueous solution

Guangze Nie[a,*], Shijun Qiu[a], Xiang Wang[a], Yan Du[a], Qingrui Zhang[b,*], Yang Zhang[a], Hengle Zhang[a]

[a] School of Environmental Science and Engineering, Nanjing Tech University, Nanjing 211816, China
[b] Hebei Key Laboratory of Heavy Metal Deep-Remediation in Water and Resource Reuse, Yanshan University, Qinhuangdao 066004, China

ARTICLE INFO

Article history:
Received 3 October 2020
Received in revised form 6 November 2020
Accepted 3 December 2020
Available online 15 December 2020

Keywords:
Molybdenum disulfide
Polystyrene host
Lead removal
Nanocomposite
Adsorption

ABSTRACT

Molybdenum disulfide (MoS_2) has excellent trapping ability for lead ions whereas its micro-/nanoscale size has greatly impeded its practical applications in the flow-through systems. Herein, a millimeter-sized nanocomposite MoS2−001 was synthesized for Pb^{2+} removal by loading MoS_2 nanosheets into a polystyrene cation exchanger D-001 by a facile hydrothermal method. The proposed structure and adsorption mechanism of MoS_2−001 was confirmed by the scanning electron microscopy (SEM), transmission electron microscopy (TEM), X-ray diffraction (XRD), and X-ray photoelectron spectroscopy (XPS) analysis. The nanocomposite showed outstanding adsorption capacity and rapid adsorption kinetic for Pb^{2+} removal, and the adsorption behavior followed the Langmuir adsorption model and pseudo-first-model kinetic model. Pb^{2+} uptake by MoS_2−001 still maintains a high level even in the presence of extremely highly competitive ions (Ca(II) and Mg(II)), suggesting its high selectivity for Pb^{2+} adsorption. Besides, the fixed-bed column experiments further certified that MoS_2−001 is of great potential for Pb^{2+} removal from the wastewater in practical engineering applications. Even more gratifying is that the exhausted MoS_2−001 can be regenerated by NaCl-EDTANa_2 solution without any significant adsorption capacity loss. Consequently, all the results indicated that MoS_2−001 is a promising candidate adsorbent for lead-containing wastewater treatment.

Wastewater containing heavy metal ions, such as Pb(II), Hg(II), Cr(VI), and Cd(II), discharged from various industries has caused a potential toxicological threat to human health [1,2]. Lead, due to its high toxicity, bioaccumulation and non-degradability has received constant attention [3,4]. The common methods for lead removal from wastewater include chemical precipitation [5], adsorption [6,7], electrocoagulation [8], and membrane filtration [9]. Among them, adsorption is considered one of the most effective treatment methods for lead-containing wastewater due to the significant advantages including low cost, high efficiency and easy handling [10–12]. However, it is still urgent to develop an adsorbent with high adsorption capacity, fast adsorption kinetics, excellent selectivity and reusability.

As a promising nanomaterial, molybdenum disulfide (MoS_2), a two-dimensional transition metal dichalcogenide (TMD), is widely favored in the fields of energy [13,14], optics [15] and electronics [16] due to its excellent electrical and mechanical properties. On the other hand, MoS_2 also shows great potential as a heavy metal adsorbent in the environmental field because of numerous active S-functional groups (considered as a potential adsorption site) on its surface, excellent chemical stability, high selectivity, and its remarkable charge transfer potential [17–20]. It has been proved that the adsorption mechanism of MoS_2 to heavy metal ions is mainly through chemical complexation to form metal-sulfur bonding [21,22]; electrostatic attraction has also been demonstrated to be a mean of adsorption [23], although its role is much less than that of complexation.

In previous studies, monolayer MoS_2 prepared by chemical exfoliation is the most optimal adsorbent for removing heavy metal ions from wastewater. However, this method will change the structure of MoS_2 [24], which need further annealing or laser to restore the original structure. In addition, there is still a bottleneck to separate and recover the monolayer MoS_2 from the liquid phase, which limits its further practical application in fixed beds or other

* Corresponding authors.
E-mail addresses: gznie@njtech.edu.cn (G. Nie), zhangqr@ysu.edu.cn (Q. Zhang).

https://doi.org/10.1016/j.cclet.2020.12.014

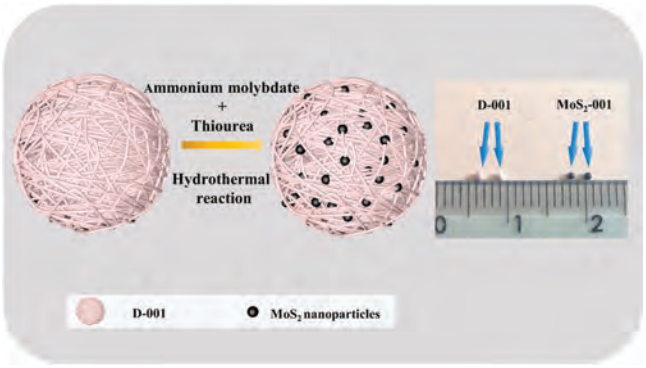

Scheme 1. The synthesis process of MoS_2-001 and optical view of D-001 and MoS_2-001.

flow-through systems for water treatment. Compared with chemical exfoliation, the hydrothermal method is more preferred due to its advantages of simple operation, large yield, controllable morphologies and facile hybridization with other functional materials [25]. The regeneration ability of an adsorbent also plays an important role during the adsorption process, but the premise is that the adsorbent is facile to be separated and recovered from water. One of the most widely used strategy for nanomaterial separation and recycle is to anchor magnetic materials on the surface of molybdenum disulfide to realize the magnetic separation of MoS_2 from the liquid phase [26–29]. Another potential strategy is to impregnate MoS_2 nanoparticles onto other porous materials with large size [30]. The large-scale host materials with built-in nanostructures could achieve highly effective solid-liquid separation. Recently, millimeter-sized ion-exchange resins have been widely employed to support nanoparticles for in the fabrication of hybrid materials because of the special merits of their satisfactory hydrodynamic performance as well as the controllable pore space and surface chemistry [31]. Meanwhile, to our knowledge, such MoS_2 hybrid material has not yet been reported.

Herein, D-001, a commercially available cation exchanger with porous polystyrene structure tailored with sulfonic acid groups [$RSO_3^-{\cdot}Na^+$] was selected as the host to load MoS_2 nanosheets by simple hydrothermal method. The basic physicochemical properties of the resultant nanocomposite (named MoS_2-001) were characterized and the effects of solution pH, reaction temperature, adsorption time and coexisting ions on lead removal were examined by batch adsorption experiments. Profit from the negatively charged sulfonic acid groups and millimeter-scale size of the host, the nanocomposite would have higher adsorption capacity and better hydraulic property compared to the bulk MoS_2. Fixed-bed adsorption and regeneration experiments were conducted in a glass column to further elucidate the practical application potential of MoS_2-001 in lead removal.

The detailed synthesis, characterization and experiment sections of MoS_2-001 were provided in Support information.

Macroscopically, MoS_2-001 is a spherical bead about 1 mm in diameter with no apparent difference from the host D-001 in appearance, while the color changed from white to black, as shown in Scheme 1. Further, the morphology and microstructure of the as-prepared material were characterized by scanning electron microscopy (SEM) and transmission electron microscopy (TEM) analysis. Figs. 1a and b show the SEM images of MoS_2-001's cross-section, as shown, the porous structure can be observed on the inner surface, which is conducive to providing more active sites and facilitating the diffusion of the target pollutant inside the adsorbent during the adsorption process [32]. Mo analysis of the MoS_2-001 after acidic digestion showed the loading amount of MoS_2 in nanocomposite was 6.2 wt% in Mo mass. The distribution of Mo and S element on the cross-section of the nanocomposite was characterized by energy-dispersive X-ray spectroscopy (EDS) mapping (Figs. 1c and d), the homogeneous distribution of molybdenum and sulfur also proved the successful loading of molybdenum sulfide on the host D-001. TEM analysis revealed that nanosized MoS_2 particles are well-dispersed on the host (Fig. 1e). The high resolution TEM (HRTEM) image of the MoS_2 nanosheet is shown in Fig. 1f, from where the (002) and (102) lattice fringes with a lattice spacing of 6.5 Å and 2.6 Å are observed. The X-ray diffraction spectra (XRD) of nanocomposite (Fig. 1g1) shows the typical diffraction peaks at $2\theta = 13.56°$, 32.29°, 35.65°and 57.65° corresponding to the (002), (100), (102) and (110) planes of MoS_2 [33,34], and matched well with the standard 2H phase of MoS_2. The

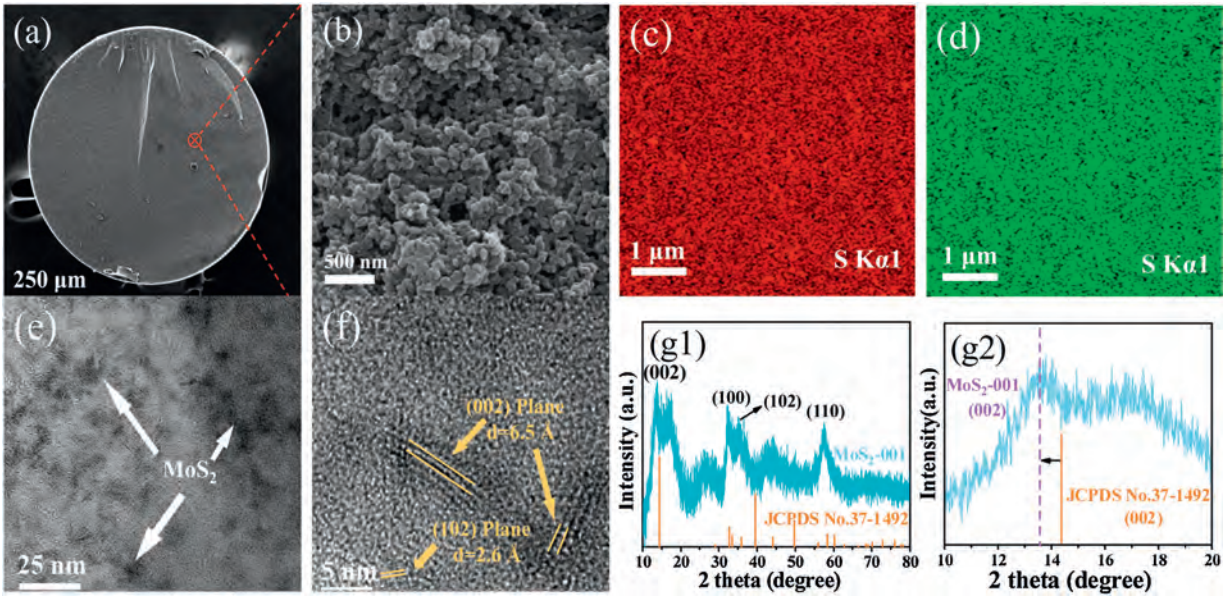

Fig. 1. Characterization of the as-prepared MoS_2-001. (a) SEM image of MoS_2-001 at cross-section, (b) the enlarged view of (a) (c and d) corresponding EDS mapping of (b, e, f) TEM and HRTEM images of MoS_2-001, (g1) XRD pattern, (g2) the (002) peak shift of MoS_2-001.

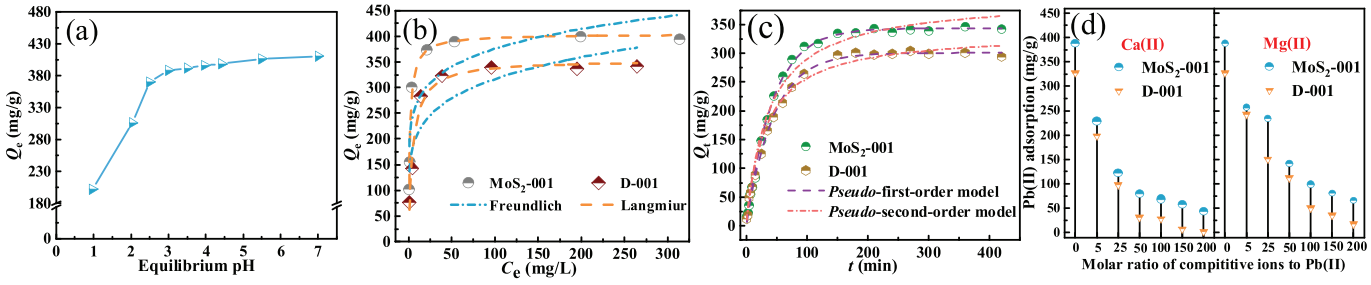

Fig. 2. (a) Effect of equilibrium pH (T = 298 K). (b) Adsorption isotherm of Pb(II) on MoS_2-001 and D-001 (pH 4.8 ± 0.2, T = 298 K). (c) Effect of contact time on Pb(II) adsorption on MoS_2-001 and D-001 (pH 4.8,T = 298 K, initial Pb(II) concentration = 200 mg/L). (d) Effect of competitive ions on Pb(II) uptake onto MoS_2-001 and D-001 (T = 298 K, pH 4.8 ± 0.2, initial Pb(II) concentration = 250 mg/L).

layer spacing of the loaded MoS_2 (~6.5 Å) was calculated by Bragg's Law (Eq. S2 in Support information), and the result is in good agreement with the HRTEM image. Particularly, due to the addition of excessive thiourea in the synthesis process, the (002) peak shift to a lower angle (Fig. 1g2), indicting the D-spacing of MoS_2-001 is larger than the standard 2H phase of MoS_2 (JCPDS No. 34-1942). It was reported that excessive sulfur element in the synthesis process can expand the layer spacing of MoS_2 [35], which is conducive to the diffusion and capture of Pb(II).

To investigate the adsorption performance of MoS_2-001 toward Pb(II), sorption experiments were conducted by the batch equilibrium method. As a pivotal factor, the solution pH has a great influence on the adsorption process. Generally speaking, the higher pH values would facilitate the Pb(II) adsorption onto MoS_2-001 (Fig. 2a). As shown, the uptake capacity increased dramatically from 201.81 mg/g to 388.10 mg/g with increasing pH from 1.0 to 3.0, then tends to be stable between pH from 3.0 to 7.0. Such pH-dependent adsorption could be explained by the specific structure of MoS_2-001: The negatively charged sulfonic groups bound on the host D-001 could sequester lead ions through nonspecific electrostatic interaction [36], and the MoS_2 nanosheets loaded on the host showed strong specific complexation with lead ions [35]. Generally, low pH value would enhance the surface protonation of MoS_2, thus increasing the repulsive force between nanomaterials and lead ions. Besides, a high concentration of hydrogen ions can compete with lead ions for adsorption sites, which is not conducive to adsorption.

Comparative study on the absorption capability of MoS_2-001 and D-001 was investigated by adsorption isotherm experiments, and the results are shown in Fig. 2b. Notably, the adsorption capacity of the nanocomposite is significantly higher than that of the host D-001 under different lead concentrations. Langmuir and Freundlich models (Text S6 in Support information) were utilized to analyze the experiment data [37,38]. As shown in Table S1 (Supporting information), the Langmuir model with a correlation coefficient as high as 0.99 can well describe the adsorption behavior of MoS_2-001, and the adsorption process suggests being monolayer adsorption. The maximum adsorption capacities of Pb (II) uptake by D-001 and nanocomposite MoS_2-001 determined from the Langmuir model are 353.79 and 404.17 mg/g, respectively. It can be inferred that the higher adsorption capacity of MoS_2-001 was attributed to the successful embedding of MoS_2 provides more potential adsorption sites for Pb(II) adsorption. In addition, we also evaluated the Pb(II) adsorption on the bulk MoS_2 under the same conditions (Fig. S1 and Table S1 in Supporting information). The maximum adsorption capacity (about 274.88 mg/g) is lower than other two samples, which may be due to the loss of active sites caused by agglomeration of MoS_2 nanoparticles. The adsorption kinetics of lead on MoS_2-001 and D-001 are depicted in Fig. 2c. The uptake of Pb(II) from aqueous solution both by MoS_2-001 and D-001 was very rapid within the initial 60 min and then slowed down considerably before gradually attaining equilibrium at 150 min. The *pseudo*-first order model and *pseudo*-second order model (Text S6) were employed to fit the adsorption kinetic data [39,40]. The results of model calculations are shown in Fig. 2c and the fitted parameters are presented in Table S2 (Supporting information). The pseudo-first order model can better describe the process of lead removal on MoS_2-001 and D-001 due to its higher correlation coefficients (R^2 = 0.998), as well as the calculated Q_e values closer to the experimental ones. The better description by the pseudo-first-order model indicated that the adsorption process is mainly controlled by the diffusion process [41]. The excellent adsorption property of MoS_2-001 can be elucidated based on its specific dual structure, *i.e.*, the sulfonic acid groups bonding to the host D-001 exerts a powerful electrostatic effect which can enhance pre-concentration and permeation of lead ions before their effective sequestration by the MoS_2 nanoparticles, known as the Donnan effect [42]. Under similar reaction conditions, adsorption on MoS_2-001 was compared with other reported materials (Table 1) [29,43–48] Apparently, MoS_2-001 has an enormous advantage both in adsorption capacity and kinetics, which can be used in the treatment of lead-containing wastewater.

There are many other cations such as Ca(II) and Mg(II) ions, usually coexist with the target ions [49]. Therefore, it is necessary to evaluate the selectivity and anti-interference of the nano-composite adsorbent for Pb(II) removal. Here, Ca(II) and Mg(II)

Table 1
Comparison of adsorption capacity for Pb(II) by different adsorbents.

Adsorbents	Temperature (K)	pH	Qm (mg/g)	Kinetics (min)	Ref.
Hydrochar/MgAl-layered double hydroxides composites	298	4.33	62.44	~750	[43]
Biowaste-derived char with amino functionalization	303	5.0	138.50	NA	[44]
Chitosan/poly (ethylene oxide) nanofibrous membrane	298	NA	108.00	~420	[45]
Multithiol functionalized graphene bio-sponge	294	5.3	101.01	~300	[46]
Hydrophilic triazine-based dendron	298	5.5	133.47	~240	[47]
Surface modified layered double hydroxide/polyaniline	298	6.0	109.71	~280	[48]
Fe_3O_4-MoS_2	298	5.0	263.6	~180	[29]
D-001	298	4.8	353.79	~150	This study
MoS_2-001	298	4.8	404.17	~150	This study

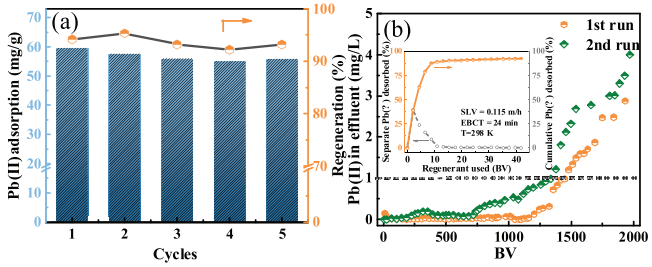

Fig. 3. (a) Cyclic adsorption-regeneration experiments (pH = 4.8, T = 298 K, Pb(II) = 50 mg/L, Ca(II) = Mg(II) = Na(I) = 200 mg/L). (b) Continuous treatment capacity evaluation for application onto MoS_2-001 during fixed-bed column runs at 298 K (Pb(II) = 10 mg/L, Ca(II) = Mg(II) = Na(I) = 200 mg/L, pH 4.8 ± 0.3, T = 298 K, EBCT = 6 min), the inset is the column regeneration of the exhausted MoS_2-001 (SLV = 0.115 m/h, EBCT = 24 min, T = 298 K).

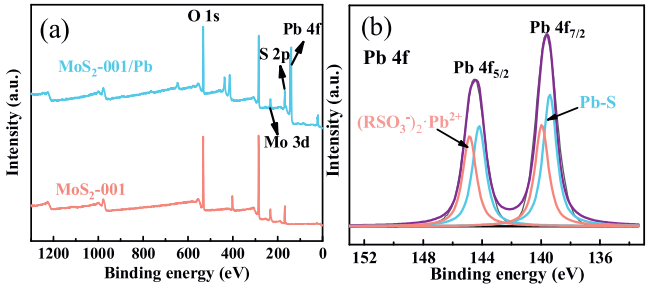

Fig. 4. (a) XPS survey spectrum of MoS_2-001 before and after Pb(II) adsorption. (b) Deconvoluted spectra of Pb 4f on the Pb(II) loaded adsorbent.

with different molar ratios to Pb(II) were selected as competitive ions, and the results were illustrated in Fig. 2d. With the increase of competing ion concentration, the adsorption capacities of MoS_2-001 and D-001 decreased significantly. However, it is worth noted that MoS_2-001 still has a decent adsorption capacity even in the presence of calcium or magnesium ions with a molar ratio of 200, while D-001 has almost no adsorption capacity under such conditions. Compared to the host D-001, the adsorption selectivity of MoS_2-001 for Pb(II) was enhanced. This may be attributed to that D-001 host captures Pb(II) ions only through the non-specific electrostatic interactions with its negatively charged sulfonic acid groups, and the common ions would compete for these adsorption sites, leading to a decrease in the adsorption capacity for Pb(II) ions. Whereas the impregnated MoS_2 in D-001 with the soft Lewis base nature from sulfide ions can selectively bond with the soft Lewis acid Pb(II) ions to form metal-sulfur complex [35,50]. To evaluate the reusability of MoS_2-001, 5 cycles of Pb(II) adsorption onto MoS_2-001 followed by regeneration with a binary 10 wt% NaCl + 0.1 mol/L EDTA-2Na solution were conducted. As illustrated in Fig. 3a, the negligible capacity loss indicated its excellent stability and reusability for Pb(II) removal.

MoS_2-001 was available in fixed-bed owe to the millimeter size of the host D-001. Fig. 3b illustrates the effluent history of the separate fixed-bed columns fed with a synthetic solution containing Pb(II) and other competing ions (Na(I), Ca(II), Mg(II)). The column breakthrough point of the effluent is set at 1 mg/L, the Chinese industrial wastewater discharge standard. As expected, the effective treatable volume of MoS_2-001 approached to ~1450 bed volume (BV). The exhausted MoS_2-001 could be well regenerated with a binary 10 % NaCl +0.1 mol/L EDTA-2Na solution (Fig. 3b inset) and still able to treat ~1350 BV of wastewater in the second run, suggesting its possible applicability in practice water treatment.

In order to explore the preliminary adsorption mechanism, X-ray photoelectron spectroscopy (XPS) was employed to study the intrinsic interaction between MoS_2-001 and Pb(II). Fig. 4a shows the XPS spectra for MoS_2-001 [12] before and after adsorption. A new peak of Pb 4f can be observed after lead removal further verifying the adsorption of Pb(II) on MoS_2-001. The low contents of Mo and S elements could be explained that the thickness of the polymer exceeds the detection limit of XPS which leads to the inner MoS_2 is difficult to be detected [51]. As illustrated in Fig. 4b, the Pb $4f_{5/2}$ and Pb $4f_{7/2}$ spectrum could be divided into two peaks, respectively. The peaks around 144.2 eV and 139.3 eV are attributable to the Pb-S complex species, whereas the peaks around 144.85 eV and 139.95 eV are attributable to the $(RSO_3^-)_2{\cdot}Pb^{2+}$ species formed between Pb(II) and sulfonic acid groups by electrostatic interaction [52,53]. Thus, the adsorption preference of MoS_2-001 toward Pb(II) can be explained by its two distinct active sites for Pb(II) uptake. One is the negatively charged sulfonic acid groups covalently binding the matrix of host D-001, and the other is MoS_2 nanosheets impregnated inside D-001. Although the competitive cations would occupy the nonspecific adsorption sites of the sulfonic acid groups and result in reduced adsorption capacity, the MoS_2 nanosheets capture Pb(II) mainly through the metal-sulfur chemical complexation (the strong soft-soft interactions of Lewis acid and base) was not significantly influenced by coexisting competitive metal ions.

In summary, a millimeter-sized nanocomposite MoS_2-001 was successfully fabricated by loading molybdenum disulfide into the cation exchanger D-001. MoS_2-001 displayed high adsorption capacity, fast adsorption kinetics, and high availability in the wide range of pH 2–7 toward Pb(II). The adsorption could be well described by the Langmuir model and the pseudo-first order kinetic model. Even better, MoS_2-001 showed remarkable adsorption capacity even in the presence of an extremely high concentration of calcium and magnesium ions. This excellent performance of MoS_2-001 could mainly be attributed to the Donnan membrane effect exerted by the sulfonic acid groups bonded to the D-001 as well as the specific complexation of MoS_2 loaded inside the D-001. Fixed-bed runs and adsorption-regeneration experiments further verified its practical application potential. These properties make MoS_2-001 an excellent candidate adsorbent for lead ions removal from wastewater.

Declaration of competing interest

The authors declare that they have no known competing financial interests or personal relationships that could have appeared to influence the work reported in this paper.

Acknowledgments

We greatly acknowledge the financial support from the National Key Research and Development Program of China (No. 2017YFE0107200), Postgraduate Research & Practice Innovation Program of Jiangsu Province (No. KYCX20_1105), NSFC (No. 21876145), the Supporting Plan for 100 Excellent Innovative Talents in Colleges and Universities of Hebei Province (No. SLRC2019041), and Open Foundation of State Key Laboratory of Pollution Control and Resource Reuse (No. PCRRF18026, Nanjing University).

References

[1] W. Liu, J. Tian, L. Chen, Y. Guo, Environ. Pollut. 220 (2017) 696–703.
[2] Y. Liu, T. Li, C. Ling, et al., Chin. Chem.Lett. 30 (2019) 2211–2215.
[3] Q. Yang, Z. Li, X. Lu, et al., Sci. Total Environ. 642 (2018) 690–700.
[4] L.N. Hu, Z.G. Ren, Chin. Chem. Lett. 20 (2009) 334–338.
[5] P. Zhang, S. Ouyang, P. Li, et al., J. Clean. Prod. 246 (2020) 118728.
[6] S. Bao, K. Li, P. Ning, et al., Appl. Surf. Sci. 393 (2017) 457–466.

[7] A. Shahat, H.M.A. Hassan, H.M.E. Azzazy, et al., Chem. Eng. J. 332 (2018) 377–386.
[8] H.J. Mansoorian, A.H. Mahvi, A.J. Jafari, Sep. Purif. Technol. 135 (2014) 165–175.
[9] P. Yenphan, A. Chanachai, R. Jiraratananon, Desalination 253 (2010) 30–37.
[10] Y. Li, M. Li, J. Zhang, X. Xu, Chin. Chem. Lett. 30 (2019) 762–766.
[11] M.I. Shariful, S.B. Sharif, J.J.L. Lee, et al., Carbohydr. Polym. 157 (2017) 57–64.
[12] M. Zhang, F. Jia, M. Dai, S. Song, Appl. Surf. Sci. 455 (2018) 258–266.
[13] X. Sun, Z. Wang, Appl. Surf. Sci. 455 (2018) 911–918.
[14] F. Chen, L. Wu, Z. Zhou, et al., Chin. Chem. Lett. 30 (2019) 197–202.
[15] S. Ridene, Superlattice. Microst. 114 (2018) 379–385.
[16] U. Khan, T.H. Kim, M.A. Khan, et al., Nano Energy 75 (2020) 104936.
[17] Z. Wang, A. Sim, J.J. Urban, B. Mi, Environ. Sci. Technol. 52 (2018) 9741–9748.
[18] C. Liu, Q. Wang, F. Jia, S. Song, J. Mol. Liq. 292 (2019) 111390.
[19] Q. Wang, L. Yang, F. Jia, Y. Li, S. Song, J. Mol. Liq. 263 (2018) 526–533.
[20] H. Wang, F. Wen, X. Li, et al., Sep. Purif. Technol. 170 (2016) 190–198.
[21] H. Tian, J. He, M. Hu, J. Colloid Interface Sci. 551 (2019) 251–260.
[22] C. Liu, S. Zeng, B. Yang, F. Jia, S. Song, J. Mol. Liq. 296 (2019) 111987.
[23] M.J. Aghagoli, M. Hossein Beyki, F. Shemirani, Food Chem. 223 (2017) 8–15.
[24] Z. Wang, B. Mi, Environ. Sci. Technol. 51 (2017) 8229–8244.
[25] L. Luo, M. Shi, S. Zhao, et al., J. Saudi. Chem. Soc. 23 (2019) 762–773.
[26] R. Li, H. Deng, X. Zhang, et al., Bioresour. Technol. 273 (2019) 335–340.
[27] Y. Song, M. Lu, B. Huang, et al., J. Alloys. Compd. 737 (2018) 113–121.
[28] J. Wang, W. Zhang, X. Yue, et al., J. Mater. Chem. A 4 (2016) 3893–3900.
[29] Z. Wang, J. Zhang, T. Wen, et al., Sci. Total Environ. 699 (2019) 134341.
[30] J. Qian, X. Gao, B. Pan, Environ. Sci. Technol. 54 (2020) 8509–8526.
[31] B. Pan, X. Zhang, Z. Jiang, et al., Polymer and polymer-based nanocomposite adsorbents for Water treatment, in: R. Das (Ed.), Polymeric Materials for Clean Water, Springer, Cham, 2019, pp. 93–119.
[32] G. Nie, L. Wu, Y. Du, et al., Chem. Eng. J. 360 (2019) 1128–1136.
[33] H. Cao, Z. Bai, Y. Li, et al., ACS Sustain. Chem. Eng. 8 (2020) 7343–7352.
[34] P. Afanasiev, C. Geantet, I. Llorens, O. Proux, J. Mater. Chem. 22 (2012) 9731–9737.
[35] K. Ai, C. Ruan, M. Shen, L. Lu, Adv. Funct. Mater. 26 (2016) 5542–5549.
[36] R.S. Juang, S.H. Lin, T.Y. Wang, Chemosphere 53 (2003) 1221–1228.
[37] Y. Du, S. Qiu, X. Zhang, G. Nie, Chem. Eng. J. 400 (2020) 125907.
[38] Y. Hu, Y. Du, G. Nie, et al., Sci. Total Environ. 700 (2020) 134999.
[39] Q. Zhang, J. Teng, Z. Zhang, et al., RSC Adv. 5 (2015) 55445–55452.
[40] C.D. Shuang, F. Yang, F. Pan, et al., Chin. Chem. Lett. 22 (2011) 1091–1094.
[41] Y.S. Ho, G. McKay, Process Biochem. 34 (1999) 451–465.
[42] S. Sarkar, P.K. Chatterjee, L.H. Cumbal, A.K. SenGupta, Chem. Eng. J. 166 (2011) 923–931.
[43] X. Luo, Z. Huang, J. Lin, et al., J. Clean. Prod. 258 (2020) 120991.
[44] Y. Liu, J. Xu, Z. Cao, et al., J. Colloid. Inter. Sci. 559 (2020) 215–225.
[45] A.A. Alqadami, M. Naushad, Z.A. Alothman, M. Alsuhybani, M. Algamdi, J. Hazard. Mater. 389 (2020) 121896.
[46] P.L. Yap, Y.L. Auyoong, K. Hassan, et al., Chem. Eng. J. 395 (2020)124965.
[47] C. Chen, Q. Chen, J. Kang, et al., J. Mol. Liq. 298 (2020) 112031.
[48] M. Dinari, S. Neamati, Colloid. Surf. A. 589 (2020) 124438.
[49] C.X. Li, J.M. Pan, J. Gao, Y.S. Yan, G.Q. Zhao, Chin. Chem. Lett. 20 (2009) 985–989.
[50] F. Jia, Q. Wang, J. Wu, Y. Li, S. Song, ACS Sustain. Chem. Eng. 5 (2017) 7410–7419.
[51] Q. Huang, J. Zhao, M. Liu, et al., J. Taiwan Inst. Chem. Eng. 86 (2018) 174–184.
[52] B. Pan, H. Qiu, B. Pan, et al., Water Res. 44 (2010) 815–824.
[53] N. Kumar, E. Fosso-Kankeu, S.S. Ray, ACS Appl. Mater. Inter. 11 (2019) 19141–19155.